

Flow Cytometric Analysis of the In Situ Accessibility of *Escherichia coli* 16S rRNA for Fluorescently Labeled Oligonucleotide Probes

BERNHARD MAXIMILIAN FUCHS,¹ GÜNTER WALLNER,^{2†} WOLFGANG BEISKER,²
INES SCHWIPPL,³ WOLFGANG LUDWIG,³ AND RUDOLF AMANN^{1*}

*Max-Planck-Institut für Marine Mikrobiologie, D-28359 Bremen,¹ Durchflußzytometrie,
GSF-Forschungszentrum für Umwelt und Gesundheit, D-85764 Neuherberg,²
and Lehrstuhl für Mikrobiologie, Technische Universität
München, D-80290 Munich,³ Germany*

Received 9 July 1998/Accepted 15 September 1998

In situ identification of whole fixed bacterial cells by hybridization with fluorescently labeled, rRNA-targeted oligonucleotide probes is often limited by low signal intensities. In addition to an impermeability of the cell periphery and a low cellular rRNA content, the three-dimensional structure of the ribosome may hinder the access of oligonucleotides to their target sites. Until now, a systematic study on the accessibility of 16S rRNA target sites had not been done. Here, we report fluorescence intensities obtained with more than 200 oligonucleotide probes (mostly 18-mers) used with whole fixed cells of *Escherichia coli* DSM 30083^T. Two overlapping sets of adjacent oligonucleotides, 171 in total, were designed to cover the full length of the 16S rRNA. The two sets are shifted by 5 to 13 nucleotides. The probes were labeled with carboxyfluorescein, and signal intensities of hybridized cells were quantified by flow cytometry. Care was taken that the signal intensity of cells was dependent solely on the in situ accessibility of probe target sites. The brightest signal resulted from probe Eco1482, complementary to positions 1482 to 1499. With this probe, the fluorescence was 1.7 times brighter than that of the standard bacterial probe EUB338 and 44 times brighter than that of the worst probe, Eco468. The distribution of probe-conferred cell fluorescence in six arbitrarily set brightness classes (classes I to VI; 100 to 81%, 80 to 61%, 60 to 41%, 40 to 21%, 20 to 6%, and 5 to 0% of the brightness with Eco1482, respectively) was as follows: I, 4%; II, 14%; III, 21%; IV, 29%; V, 19%; and VI, 13%. A more detailed analysis of helices 6, 18, and 23 with additional probes demonstrated that a shift of the target region by only a few bases could result in a decline of cell fluorescence from >80 to <10%. Considering the high evolutionary conservation of 16S rRNA, the in situ accessibility map of *E. coli* should facilitate a more rational selection of probe target sites for other species as well.

In situ hybridization with fluorescently labeled, rRNA-targeted oligonucleotide probes, originally introduced to microbiology by DeLong and coworkers in 1989 (8), has become a much-used and important technique over the last decade (4). It is an integral part of the rRNA approach to microbial ecology and evolution (20) and enables the in situ identification of individual microbial cells in complex environmental samples. Originally restricted to a few expert laboratories, the increasing availability of 16S rRNA sequences (17, 29) brought rRNA-targeted probing within the reach of many laboratories. Software for rational probe design, such as the ARB package (27), has been developed, allowing for a rapid and directed selection of target sites for specific species or other taxonomic units. Furthermore, >100 µg of fluorescently labeled oligonucleotide probes, sufficient for several thousand hybridizations, can today be supplied within a few days for less than \$100.

Soon after the introduction of in situ hybridization to microbiology, it was realized that in addition to the cellular ribosome content and cell wall permeability, the in situ accessibility of the target site determined the probe-conferred fluorescence. About one of two newly designed probes failed, even in cases

where binding of a positive control, such as the general bacterial probe EUB338 (2), had demonstrated the presence of sufficient target rRNA and good permeation of cells of interest. A nonsystematic but quite successful approach to address the problem of variable in situ accessibility was to target new probes to sites that were known to be open in other species (4). The rationale behind this extrapolation comes from the high evolutionary conservation of the ribosome and the rRNA molecules (33). So far only a few preliminary studies have tried to address the variable accessibility of 16S rRNA, by either oligonucleotide binding assays on filters (13, 15) or fluorescent in situ hybridization (11). A systematic study was lacking.

We here report the results of the flow cytometric quantification of fluorescent signals conferred by over 200 carboxyfluorescein-labeled oligonucleotides targeted to the 16S rRNA of *Escherichia coli*. The 16S rRNA was probed with two sets of adjacent oligonucleotides, mostly 18-mers, which were shifted relative to each other by 5 to 13 nucleotides. The evolutionarily less conserved helices 6, 18, and 23 (helix numbering according to ARB [27]), which frequently allow for the design of species- or genus-specific probes, were studied at a higher spatial resolution with additional oligonucleotide probes.

MATERIALS AND METHODS

Microorganisms and fixation. For in situ hybridization the following strains were grown as described in the respective catalogues of strains: *E. coli* K-12 DSM 30083^T (Deutsche Sammlung von Mikroorganismen und Zellkulturen, Braunschweig, Germany), *Comamonas testosteroni* DSM 50244^T, *Zoogloea ramigera*

* Corresponding author. Mailing address: Celsiusstr. 1, D-28359 Bremen, Germany. Phone: 49 421 2028 930. Fax: 49 421 2028 790. E-mail: ramann@mpi-bremen.de.

† Present address: Hoechst Marion Roussel, Quality Operations Microbiology, D-65926 Frankfurt am Main, Germany.

TABLE 1. Sequences and relative fluorescence intensities of all probes used in this study

Probe name	<i>E. coli</i> position ^a		Probe sequence (5'→3')	Relative probe fluorescence (% Eco1482) ^b	Brightness class ^c
	5'	3'			
Eco1	1	19	TGATCAAACCTCTCAATTT	1	VI
Eco13	13	31	CAATCTGAGCCATGATCAA	35	IV
Eco20	20	37	AGCGTTCAATCTGAGCCA	44	III
Eco32	32	47	GCCTGCCGCCAGCGTT	42	III
Eco38	38	54	GTGTTAGGCCTGCCGCC	68	II
Eco48	48	65	TCGACTGCATGTGTTAG	76	II
Eco55	55	72	TTACCGTTCGACTTGCAT	56	III
Eco60	60	77	TCCTGTACCCTTCGACT	66	II
Eco63	63	80	GCTTCTGTACCCTTCG	67	II
Eco66	66	83	GCTGCTTCTGTTACCGT	62	II
Eco70	70	88	AGCAAGCTGCTTCTGTTA	48	III
Eco73	73	90	GCAGCAAGCTGCTTCTG	27	IV
Eco79	79	96	TTCCAGTAGTATATCC	3	VI
Eco84	84	101	TCGTACGAAAGCAGCAA	6	V
Eco87	87	104	CACCTGTACGAAAGCAG	10	V
Eco89	89	106	GCCACTCGTCAGCAAAGC	41	III
Eco91	91	108	CCGCCACTCGTCAGAAA	70	II
Eco102	102	118	ACTCACCCCTCCGCCAC	46	III
Eco109	109	126	CAGACATACTCACCCGT	40	IV
Eco119	119	136	GGCAGTTCCTCCAGACATT	27	IV
Eco127	127	144	CTCCATCAGGCAGTTC	47	III
Eco137	137	154	AGTTATCCCCCTCCATCA	35	IV
Eco145	145	162	TTCCAGTAGTATATCC	66	II
Eco155	155	172	TTAGCTACCGTTTCCAGT	46	III
Eco163	163	180	ATGCGGTATTAGCTACCG	30	IV
Eco173	173	190	TTGCGACGTTATGCGGTA	39	IV
Eco181	181	198	CTTTGGTCTTTCGACGTT	65	II
Eco191	191	209	AAGTCCCCCTCTTTGGTC	76	II
Eco199	199	215	GGCCCTAAGCTCCCCCT	61	II
Eco210	210	226	CGATGGCAAAGAGGCCCG	5	VI
Eco216	216	233	GCACATCCGATGGCAAGA	21	IV
Eco227	227	243	TCCCATCTGGGCACATC	26	IV
Eco234	234	251	CTAGCTAATCCCATCTGG	27	IV
Eco244	244	261	ACCCCACTACTAGCTAA	41	III
Eco252	252	268	AGCCGTACCCCACTA	62	II
Eco262	262	279	TGCGTACGGTAGCCGTT	19	V
Eco269	269	285	GGATCGTCGCCTAGGTG	27	IV
Eco280	280	297	CAGACAGCTAGGGATCG	25	IV
Eco285	285	302	CCTCTCAGACCAGTAGG	53	III
Eco298	298	315	TGTGGCTGGTTCCTCT	56	III
Eco303	303	320	TCCAGTGTGGCTGTTCAT	25	IV
Eco316	316	333	ACCGTGTCTCAGTTCAG	62	II
Eco321	321	338	TCTGGACCGTGTCTCAGT	71	II
Eco334	334	350	CTCCCGTAGGAGTCTGG	27	IV
Eub338	338	353	GCTGCCTCCGATAGGAGT	58	III
Eco343	343	359	CACGTCTCCCTCCCGTA	64	II
Eco351	351	369	CAATATCCCCACTGCTGC	33	IV
Eco360	360	377	CCATTGTGCAATATTC	35	IV
Eco370	370	386	GGCTTGCGCCATTGTG	52	III
Eco378	378	394	CTGCATCAGGCTTGC	32	IV
Eco387	387	403	GCGGCATGGCTGCATCA	39	IV
Eco395	395	412	TTCATACCCCGGCATGG	35	IV
Eco404	404	421	AAGGCCCTTCTCATAAC	37	IV
Eco413	413	429	TACAACCCGAAGGCCTTC	62	II
Eco422	422	439	AAAGTACTTTACAACCCG	37	IV
Eco431	431	448	TCCCGCTGAAAGTACTT	42	III
Eco439	439	455	CCCTTCTCCCGCTGA	53	III
Eco440	440	456	TCCCTTCTCCCGCTG	83	I
Eco443	443	460	TTACTCCCTTCTCCCG	62	II
Eco446	446	463	ACTTTACTCCCTTCTCC	64	II
Eco449	449	467	ATTAACCTTACTCCCTTCC	35	IV
Eco455	455	473	AAAGGTATTAACCTTACTC	3	VI
Eco468	468	486	AACGTCAATGAGCAAAGGT	3	VI
Eco474	474	491	CGGGTAACGTCAATGAGC	3	VI
Eco478	478	495	TCTGCGGGTAACGTCAAT	20	V
Eco481	481	498	TCTTCTGCGGGTAAACGT	21	IV
Eco484	484	501	GCTTCTTCTGCGGGTAAAC	60	III
Eco487	487	504	GGTGTCTTCTGCGGGT	54	III
Eco492	492	509	TAGCCGGTGTCTTCTG	46	III

Continued

TABLE 1—Continued

Probe name	<i>E. coli</i> position ^a		Probe sequence (5'→3')	Relative probe fluorescence (% Eco1482) ^b	Brightness class ^c
	5'	3'			
Eco499	499	516	ACGGAGTTAGCCGGTGCT	25	IV
Eco505	505	522	GCTGGCACGGAGTTAGCC	56	III
Eco510	510	527	CGGTGCTGGCACGGAGT	37	IV
Eco523	523	540	CTCCGTATTACCGCGGCT	54	III
Eco528	528	545	GCACCCTCCGTATTACCG	42	III
Eco541	541	558	CCGATTAACCGTTGCACC	96	I
Eco548	548	566	CAGTAATTCGATTAACGC	42	III
Eco559	559	576	GCTTTACGCCAGTAATT	46	III
Eco567	567	584	CTGCGTGCCTTACGCC	44	III
Eco577	577	594	AACAACCCGTCGCTGC	42	III
Eco585	585	602	TCTGACTTAACAAACCGC	2	VI
Eco595	595	613	GGGATTCACATCTGACTT	2	VI
Eco603	603	620	GAGCCCGGGGATTTTACA	4	VI
Eco614	614	631	GTTCCAGTTGAGCCCG	25	IV
Eco621	621	638	AGATGCAGTTCACAGGTT	2	VI
Eco627	627	644	AGTATCAGATGCAGTTC	1	VI
Eco632	632	649	TTGCCAGTATCAGATGCA	2	VI
Eco639	639	656	CTCAAGCTTGCCAGTATC	4	VI
Eco645	645	662	ACGAGACTCAAGCTTGCC	22	IV
Eco650	650	667	CCTCTACGAGACTCAAGC	13	V
Eco654	654	671	CCCCCTTACAGAGACTC	17	V
Eco657	657	674	CTACCCCTTCTACGAGA	19	V
Eco661	661	678	AATTCTACCCCTCTAC	22	IV
Eco665	665	682	CTGGAATTCTACCCCT	21	IV
Eco668	668	685	CACCTGGAATTCTACCC	12	V
Eco675	675	692	ACCGTACACCTGGAATT	50	III
Eco681	681	698	CATTTACCCGCTACACCT	55	III
Eco686	686	703	CTACGCATTTACCGCTA	40	IV
Eco690	690	707	ATCTCTACGCATTTACCC	60	III
Eco693	693	710	CAGATCTCTACGATTTTC	29	IV
Eco704	704	721	CGGTATTCTCCAGATCT	38	IV
Eco711	711	728	TCGCCACCGGTATTCCTC	62	II
Eco722	722	737	GGGCCGCTTTCGCTC	21	IV
Eco729	729	744	GTCCAGGGGGCCCT	27	IV
Eco738	738	755	CGTCAGTCTTCGTCCAGG	19	V
Eco745	745	762	ACCTGAGCGTCAGTCTTC	19	V
Eco756	756	773	CACGCTTTCGACCTGAG	15	V
Eco763	763	780	TGCTCCCCACGCTTTCGC	77	II
Eco774	774	791	CTAATCTGTTTGTCTCC	52	III
Eco781	781	799	CAGGGTATCTAATCTGTT	4	VI
Eco792	792	809	CGTGGACTACCAAGGTAT	2	VI
Eco800	800	817	GTTTACGGCGTGGACTAC	31	IV
Eco810	810	827	AGTCGACATCGTTTACCG	38	IV
Eco818	818	835	AACCTCCAAGTCGTCATC	10	V
Eco828	828	845	TCAAGGGCACAACTCCA	6	V
Eco836	836	852	CCACGCTCAAGGGGAC	8	V
Eco846	846	862	GCTCCGGAAGCCACGCC	42	III
Eco853	853	870	ACGCGTTAGCTCCGGAAG	52	III
Eco863	863	880	GGTCGACTTAACCGGTTA	42	III
Eco871	871	888	CCCCAGCGGTCGACTTA	87	I
Eco881	881	897	GGCCGTACTCCCAAGC	77	II
Eco889	889	906	TAACCTTGCAGCGCTACT	85	I
Eco898	898	916	ATTTGAGTTTTAACCTTGC	73	II
Eco907	907	925	CGTCAATTCATTGAGTTT	40	IV
Eco917	917	933	CGGGCCCCGTCATTC	69	II
Eco926	926	941	CGTGTGCGGGCCCC	38	IV
Eco934	934	951	CATGCTCCACCGTGTG	50	III
Eco942	942	959	TTAAACCACATGCTCCAC	46	III
Eco952	952	969	TTGCATCGAATTAACCA	4	VI
Eco960	960	977	TCTTCGCGTTGATCGAA	60	III
Eco970	970	987	CAGGTAAGGTTCTTCGCG	33	IV
Eco978	978	995	GTCAGACAGGTAAGGT	27	IV
Eco988	988	1005	TTCCGTGGATGTCAAGAC	8	V
Eco996	996	1013	CTGAAAATCTCCGTTGAT	10	V
Eco1006	1006	1023	ATTCTCATCTGAAAAC	4	VI
Eco1014	1014	1031	GAAGGCACATTTCAATCT	8	V
Eco1024	1024	1041	CACGGTCCCCGAAGGCAC	31	IV
Eco1032	1032	1049	ACCTGTCTCACGGTTCCC	52	III
Eco1042	1042	1059	GCCATGCAGCACCTGTCT	48	III
Eco1050	1050	1067	TGACGACAGCCATGCAGC	6	V

Continued on following page

TABLE 1—Continued

Probe name	<i>E. coli</i> position ^a		Probe sequence (5'→3')	Relative probe fluorescence (% Eco1482) ^b	Brightness class ^c
	5'	3'			
Eco1060	1060	1077	CAACACGAGCTGACGACA	2	VI
Eco1068	1068	1085	ACATTTACACAACACGAGC	12	V
Eco1078	1078	1095	ACTTAACCCAACATTTCA	6	V
Eco1086	1086	1103	GTTGCGGACTTAACCCA	10	V
Eco1097	1097	1112	GTTGCGTCTGTTGCGGG	6	V
Eco1104	1104	1121	AGGATAAGGGTTGCGCTC	8	V
Eco1113	1113	1130	TGGCAACAAAGGATAAAG	2	VI
Eco1122	1122	1139	CCGGACCGCTGGCAACAA	15	V
Eco1131	1131	1146	TTCCCGGCGGACCGC	40	IV
Eco1140	1140	1157	TCTCTTTGAGTTCGGG	46	III
Eco1147	1147	1165	ACTGGCAGTCTCCTTTGAG	13	V
Eco1158	1158	1175	CCAGTTTACTACTGGCAG	2	VI
Eco1166	1166	1183	ACCTTCTCCAGTTTATC	10	V
Eco1176	1176	1193	CGTCATCCCCACCTTCTC	50	III
Eco1184	1184	1201	TGACTTGACGTCATCCCC	6	V
Eco1194	1194	1211	AGGGCCATGATGACTTGA	10	V
Eco1202	1202	1219	TGGTCGTAAGGGCCATGA	2	VI
Eco1212	1212	1229	TGTGTAGCCCTGGTCGTA	25	IV
Eco1220	1220	1237	GTAGCAGCTGTGTAGCC	58	III
Eco1230	1230	1247	AGTCCGCTTGTAGCAGC	35	IV
Eco1238	1238	1255	CTCTTTGTATGCGCCATT	31	IV
Eco1248	1248	1265	GAGGTCGCTTCTTTTGT	58	III
Eco1256	1256	1273	GCTCTCGGAGGTCGCTT	62	II
Eco1266	1266	1283	AGTCCGCTTGTCTTCGC	58	III
Eco1274	1274	1291	ACTTTATGAGGTCGCTT	15	V
Eco1284	1284	1301	ACTACGACGCACTTTATG	15	V
Eco1292	1292	1309	CAATCCGGACTACGACGC	23	IV
Eco1302	1302	1319	TTGCAGACTCCAATCCGG	33	IV
Eco1310	1310	1327	GAGTCGAGTTGACGACTC	2	VI
Eco1320	1320	1337	CAGCTTACTGGAGTCGAG	6	V
Eco1328	1328	1345	AGCGATTCCGACTTTCATG	65	II
Eco1338	1338	1355	CACGATTACTAGCGATTCC	15	V
Eco1346	1346	1363	TTCTGATCCACGATTACT	12	V
Eco1356	1356	1373	CACCGTGGCATTCTGATC	19	V
Eco1364	1364	1382	GAACGATTACACCGTGGCA	21	IV
Eco1374	1374	1391	AAGGCCCGGAACGTATT	52	III
Eco1383	1383	1400	GGTGTGTACAAGGCCCGG	65	II
Eco1392	1392	1409	GTCAGCGGCGGTGTGTAC	67	II
Eco1401	1401	1418	TCCCATGGTGTGACGGGC	67	II
Eco1410	1410	1427	GCAACCCACTCCATGGT	90	I
Eco1419	1419	1436	ACTTCTTTTGCAACCCAC	23	IV
Eco1428	1428	1445	AAGTACTACTTCTTTT	38	IV
Eco1437	1437	1454	CCGAAGTTAAGTACCT	4	VI
Eco1446	1446	1463	AGCGCCCTCCCGAAGGT	4	III
Eco1455	1455	1472	AAAGTGTAAAGCGCCCTC	31	IV
Eco1464	1464	1481	ATGAATCACAAAGTGGTA	4	VI
Eco1473	1473	1490	ACCCAGTCATGAATCAC	65	II
Eco1482	1482	1499	TACGACTTCACCCAGTC	100	I
Eco1491	1491	1508	TTACTCTTGTACGACTTC	31	IV
Eco1500	1500	1517	CCCTACGGTTACTCTTGT	92	I
Eco1509	1509	1525	CGCAGGTTCCCTACGG	4	VI
Eco1518	1518	1535	GTGATCCAACCGAGGTT	17	V
Eco1526	1526	1542	TAAGGAGGTGATCCAAC	25	IV

^a *E. coli* positions according to the numbering of Brosius et al. (7).

^b Fluorescence intensities expressed as percentages of that for the brightest probe detected, Eco1482.

^c Probes were grouped according to their relative fluorescence into six classes of brightness: class I (100 to 81% relative fluorescence compared to Eco1482), class II (80 to 61%), class III (60 to 41%), class IV (40 to 21%), class V (20 to 6%), and class VI (5 to 0%).

ATCC 25935 (American Type Culture Collection, Rockville, Md.), and *Acinetobacter calcoaceticus* DSM 30006^T. Cells were harvested in logarithmic growth phase (optical density at 600 nm, ~0.5), washed once with 1× phosphate-buffered saline (1× PBS) (130 mM sodium chloride, 10 mM sodium phosphate buffer, pH 7.2), and fixed with 4% paraformaldehyde as described previously (3).

Sequencing. Almost-full-length (positions 7 to 1542) 16S ribosomal DNA (rDNA) of *E. coli* K-12 DSM 30083^T was amplified directly from freshly harvested cells by PCR as described previously (32). After subsequent purification with a QIAquick PCR purification kit (Qiagen, Hilden, Germany), both strands of the PCR product were sequenced with a 377 DNA sequencer with the PRISM

Dye Terminator Cycle Sequencing Ready reaction kit (Perkin-Elmer, Applied Biosystems, Foster City, Calif.) supplied with AmpliTaq DNA polymerase in order to verify that all probes were indeed targeted to fully complementary target sites. As expected, the determined sequence was identical to that deposited at the EMBL database under accession no. X80725.

Probe design. Oligonucleotide probes were designed to be complementary to the sequence determined from *E. coli* DSM 30083^T. Two sets of adjacent oligonucleotide probes were designed, with the first set covering the full length of the 16S rRNA from position 1 to 1542 and the second set shifted by 5 to 13 nucleotides and complementary to positions 13 to 1535. Probes specific for microheterogeneities in the 16S rRNA operons *rmH* (accession no. D12649 and D15061), *rmG* (V00348), *rmD* (M24911), *rmA* (M87049), *rmB* (J01695), *rmE* (U00006), and *rmC* (L10328) in *E. coli* K-12 were developed based upon the EMBL sequences. The standard probe length was 18 nucleotides. If the theoretical melting point according to the 4+2 formula of Suggs et al. (28), $T_d = [4 \cdot (G+C) + 2 \cdot (A+T)]$, was above 60°C or below 48°C, the probe length was varied accordingly. All probes, with their sequences and target positions, are listed in Table 1.

Probe labeling and quality control. Probes were synthesized, monolabeled at the 5' end with 5-(6)-carboxyfluorescein in the last step of solid-phase synthesis, and purified by high pressure liquid chromatography by Interactiva GmbH (Ulm, Germany). Since differences in the quality of labeling directly influenced the amount of probe-conferred fluorescence (data not shown), aliquots of each probe were analyzed in a spectrophotometer (DU650; Beckmann, Munich, Germany). Absorption peaks at 496 nm (carboxyfluorescein) and 260 nm (oligonucleotide) were recorded. According to the Beer-Lambert law, the ratio of absorption at 496 nm (A_{496}) to A_{260} for a monolabeled oligonucleotide should match the ratio of the extinction coefficients (ϵ) of carboxyfluorescein and oligonucleotide. The extinction coefficient at 260 nm (ϵ_{260}) of an oligonucleotide can be estimated from its nucleotide composition as the sum of the extinction coefficients of the individual nucleotides (dATP, 15.4 cm² μmol⁻¹; dCTP, 7.3 cm² μmol⁻¹; dGTP, 11.7 cm² μmol⁻¹; and dTTP, 8.8 cm² μmol⁻¹) (23). With the ϵ_{496} of carboxyfluorescein taken as 75 cm² μmol⁻¹, we estimated the quality of oligonucleotide labeling by calculating a ratio, k , according to the following formula: $k = (\epsilon_{260}/\epsilon_{496})/(A_{260}/A_{496})$. k values of <1 indicate an incomplete labeling of a probe, whereas values of >1 point to the presence of additional, potentially unbound carboxyfluorescein. Considering inaccuracies in the estimation of the extinction coefficients of oligonucleotides, we accepted k values of between 0.7 and 1.3, assuming that these oligonucleotides were monolabeled.

Fluorescent in situ hybridization. Fixed cells at an approximate final concentration of 10⁶ μl⁻¹ were hybridized in 100 μl of buffer containing 0.9 M sodium chloride, 0.1% sodium dodecyl sulfate, 20 mM Tris-HCl (pH 7.2), and 1.5 ng of fluorescent probe μl⁻¹ at 46°C for 3 h (31). Subsequently, cells were pelleted by centrifugation for 2 min at 4,000 × *g* and resuspended in 100 μl of hybridization buffer containing no probe. After washing for 30 min at 46°C, samples were mixed with 500 μl of 1× PBS (pH 8.4), immediately placed on ice, and analyzed within 3 h.

To investigate whether different dissociation temperatures influenced the probe-conferred fluorescence, hybridization stringencies were altered for a subset of probes by changing the concentrations of formamide and sodium chloride in the buffer as described earlier (26). At a fixed hybridization temperature of 46°C, stringency was adjusted by adding either sodium chloride, assuming that concentrations of 1.8 and 3.6 M would be equivalent to hybridizations in the standard hybridization buffer at 41 and 36°C, respectively, or formamide, assuming an increase of the effective hybridization temperature of 0.5°C per 1% of added formamide (26).

Flow cytometry. The fluorescence intensities of hybridized cells were quantified with a FACStar Plus flow cytometer (Becton Dickinson, Mountain View, Calif.). The 488-nm emission line of an argon ion laser was used as the light source and tuned to an output power of 200 or 300 mW. Forward-angle light scatter (FSC) and right-angle light scatter (SSC) were both detected with a BP 488/10 (Becton Dickinson) band-pass filter. Fluorescence (FL1) was detected with a DF 530/30 band-pass filter. Because of lower background signals, the system threshold was usually set on SSC. Since the fluorescence of carboxyfluorescein is pH sensitive, care was taken that the sheath fluid (1× PBS) always had a pH of 8.4. All measurements were calibrated to green-fluorescent, 0.5-μm polystyrene beads (catalogue no. 17152; Polysciences, Warrington, Pa.) to check the stability of the optical alignment of the flow cytometer and to standardize the fluorescence intensities of the probes.

Data acquisition and processing. The parameters FSC, SSC, and FL1 were recorded as pulse height signals (four orders of magnitude), and for each measurement 10,000 events were stored in list-mode files. Subsequent analysis was done with CellQuest software (Becton Dickinson) and with the DAS software package (6). Probe-conferred fluorescence was determined as the median of the FL1 values of single cells lying in a gate that was defined in an FSC-versus-FL1 dot plot. Fluorescence of cells was corrected by subtraction of background fluorescence of negative controls and standardized to the fluorescence of reference beads. All values were finally expressed relative to that for the brightest probe detected.

Probe-conferred fluorescence intensities of triplicate samples were recorded. Each replicate represents an independent cell preparation and hybridization. Only triplicates with a coefficient of variation of less than 10% were accepted; otherwise, the quantification was repeated. To compensate for daily variations in

sample preparation and flow cytometer performance, measurements with each probe were done in at least three independent experiments with three parallel hybridizations each. The means of the three triplicate measurements are given in Table 1. No standard deviations are given there, since the coefficients of variation in all cases were <10%.

RESULTS

Optimization of sample treatment. Considerable effort was spent on optimizing each step of the hybridization procedure before starting the systematic study. The in situ hybridization protocol was adapted from that described by Wallner et al. (31), but the following parameters were reevaluated for selected probes.

(i) **Probe concentration.** Hybridizations with probes Eco431 and Eco440 at final concentrations of 1, 2, and 4 ng μl^{-1} (assuming that 1 optical density unit at 260 nm = 20 ng μl^{-1}) yielded fluorescence intensities of hybridized cells that were identical within the variation limits. At a concentration of 8 ng μl^{-1} , fluorescence intensities were increased, probably due to nonspecific staining (data not shown). In order to save probe and to rule out an influence of small differences in the probe concentrations, all further experiments were performed at 1.5 ng μl^{-1} .

(ii) **Cells.** For concentrations of 1×10^6 to 8×10^6 cells μl^{-1} of hybridization buffer⁻¹, no effect on the specific fluorescence signals could be detected. Accordingly, concentrations of fixed cells were kept in this range. In another preliminary experiment, we tried to analyze whether the in situ accessibility of *E. coli* DSM 30083^T cells fixed from stationary growth phase was different from that of cells fixed from logarithmic phase. Fluorescence intensities were determined for 17 representatively chosen probes. As expected, stationary-growth-phase cells showed clearly lower absolute signal intensities for all probes, most likely due to their lower ribosome content, but the relative intensities of the probes were approximately the same as for log-phase cells (data not shown). Consequently, for further accessibility studies only cells in logarithmic growth phase were used.

(iii) **Storage.** Due to the large number of samples processed per day (>100), the time between the analysis of the first and last samples could be up to 5 h. Reanalysis of samples stored on ice proved that no significant loss of cellular fluorescence occurred during this period. Even after 30 h of storage, signals were stable for probes Eco66, Eco440, and Eub338 and decreased by only about 25% for probes Eco55 and Eco91 (data not shown).

Influence of probe-specific differences in dissociation temperatures on probe-conferred fluorescence. The signal conferred by a nucleic acid probe is strongly dependent on the hybridization stringency. It was therefore crucial for this study to consider the effect of probe-to-probe variation in thermal stability. An initial precaution to guarantee maximum and, at the same time, specific binding of all probes was a restriction to probes with theoretical T_d values of between 48 and 60°C and a standard hybridization temperature of 46°C. However, T_d estimation by the 4+2 formula is only a rough approximation, and we therefore analyzed nine probes at various hybridization stringencies. The stringency-binding plots showed in general the typical sigmoid shape, with a transition zone connecting a low-stringency region with strong binding to a high-stringency zone with weak binding (Fig. 1). As expected, seven probes showed maximum fluorescence intensities at the standard hybridization temperature of 46°C. However, probes Eco431 ($T_d = 54^\circ\text{C}$ by the formula of Suggs et al. [28]) and Eco449 ($T_d = 52^\circ\text{C}$) had their maximum fluorescence at 41°C and showed 80 and 79%, respectively, of maximum binding at

46°C. Nevertheless, we continued to use our standard hybridization temperature of 46°C and did not choose a lower hybridization temperature, because some probes exhibited lower signal intensities at lower temperatures. For instance, probes Eco91 and Eco145 at 41°C showed only 84 and 90%, respectively, of their signal intensities at 46°C.

Operon diversity. The standard set of oligonucleotide probes was designed to be complementary to a 16S rDNA sequence of *E. coli* DSM 30083^T. To ensure a correct basis for probe design, the sequence was confirmed by sequencing the 16S rDNA of the batch of cells used in this study, and it was found that the sequences were indeed identical (data not shown). Sequence comparison of the *E. coli* DSM 30083^T 16S rDNA sequence used in this study for probe design with the published sequences of the seven *E. coli* K-12 rRNA operons revealed that three operons, *rmH*, *rmA*, and *rmC*, showed a few differences in four regions. A total of 20 probes targeting these regions were redesigned to be complementary to the sequences of specific operons. However, none of the probes yielded higher fluorescence intensities than the standard probe set, and also the combined use of the operon-specific probe and the respective probe from the standard set did not result in higher signals (data not shown).

Accessibility of the 16S rRNA for fluorescently labeled oligonucleotide probes. The results of the flow cytometric quantification of the fluorescence intensities conferred by the two adjacent sets of oligonucleotides are listed in Table 1. The brightest fluorescence resulted from probe Eco1482, targeting positions 1482 to 1499. The fluorescence was 1.7 times brighter than that with the frequently used bacterial probe EUB338 and 44 times brighter than that with probes which yielded only background fluorescence, e.g., Eco468. In Table 1 fluorescence intensities of all probes are expressed as percentages of that of Eco1482. Furthermore, all probes were arbitrarily grouped according to their relative fluorescences into six classes of brightness: class I (100 to 81% of the fluorescence of Eco1482), class II (80 to 61%), class III (60 to 41%), class IV (40 to 21%), class V (20 to 6%), and class VI (5 to 0%). Figure 2 shows the distribution of the different brightness classes over the 16S rRNA secondary structure model (12).

Of a total of 171 probes, only 7, i.e., Eco440 (83%), Eco541 (96%), Eco871 (87%), Eco889 (85%), Eco1410 (90%), Eco1482 (100%), and Eco1500 (92%), are in the brightest class, class I, and 24 belong to class II. Most probes in these two classes are directed against five regions where accessibility for oligonucleotide probes in *E. coli* seems to be very high: (i) positions 38 to 108 (5' halves of helices 4, 5, and 6 and 3' half of helix 6), except for the terminal loop region of helix 6 (see below for details); (ii) positions 181 to 215 (helix 10 and 5' half of helix 11); (iii) positions 316 to 359 (helix 14 and 3' halves of helices 15 and 5), except for Eco334 and EUB338 target positions; (iv) positions 871 to 933 (3' halves of helices 27 and 20, helix 30, and 5' half of helix 31); and (v) positions 1383 to 1427 and 1473 to 1517 (the proximal part of helix 49 including the 3' half of helix 31 and the 5' half of helix 50). Nine smaller hot spots are spread over the whole 16S rRNA. About half of all of the probes are in classes III (36 probes) and IV (49 probes), which include probes that are as bright as EUB338 (58% of Eco1482 brightness). The signal-to-noise ratios even for the less bright probes of class IV were still >8 for log-phase *E. coli* cells.

One-third of all of the probes showed weak or no signals (classes V and VI; 0 to 20% of Eco1482 fluorescence). Apparently totally blocked sites (class VI) include the 5' end of the 16S rRNA; the 3' half of helix 11; the loop region and the 3' half of helix 18; almost the complete helix 22; the loop regions of helices 26, 37, 45, 47, and 50; and the target sites of probes

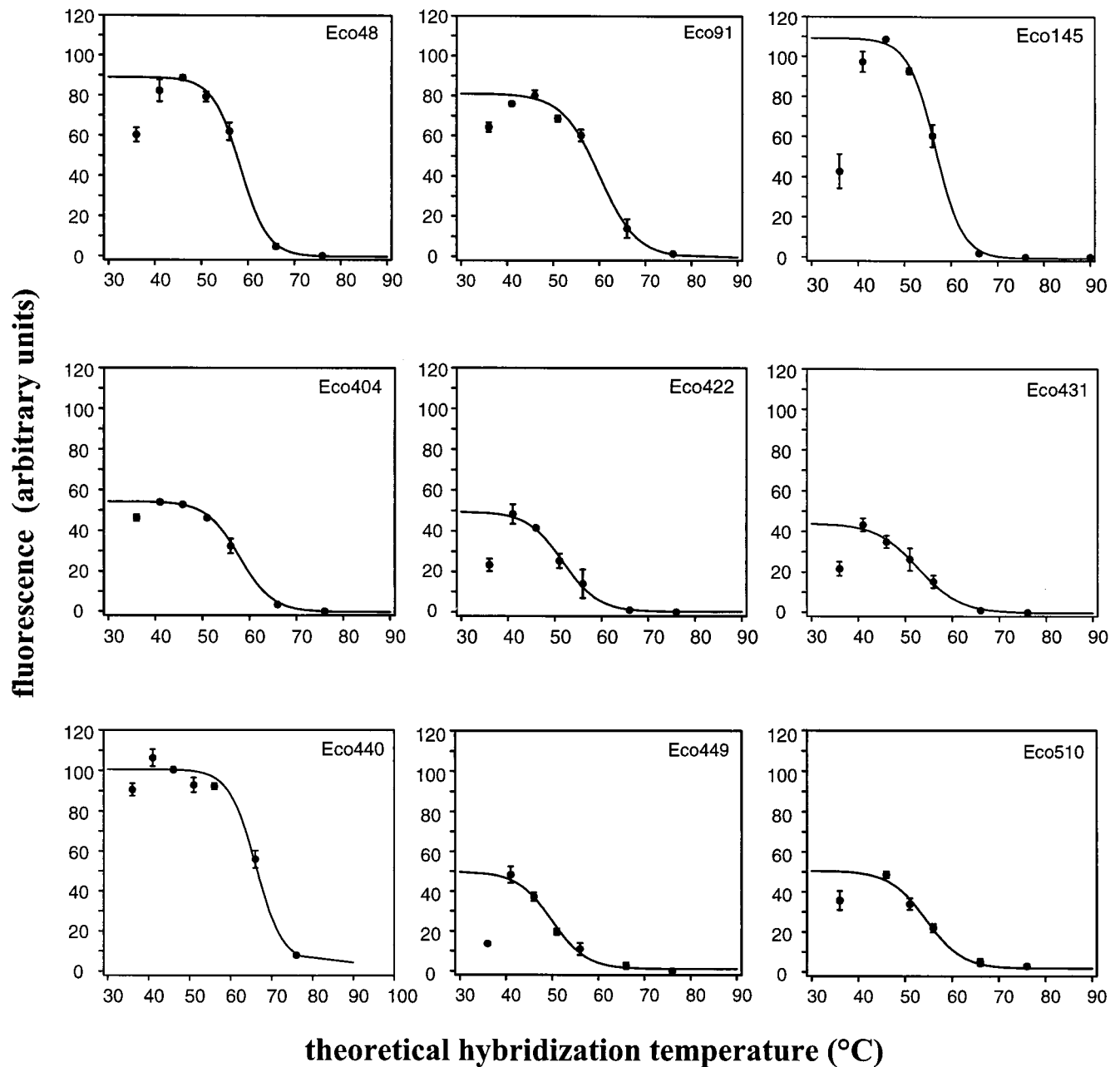


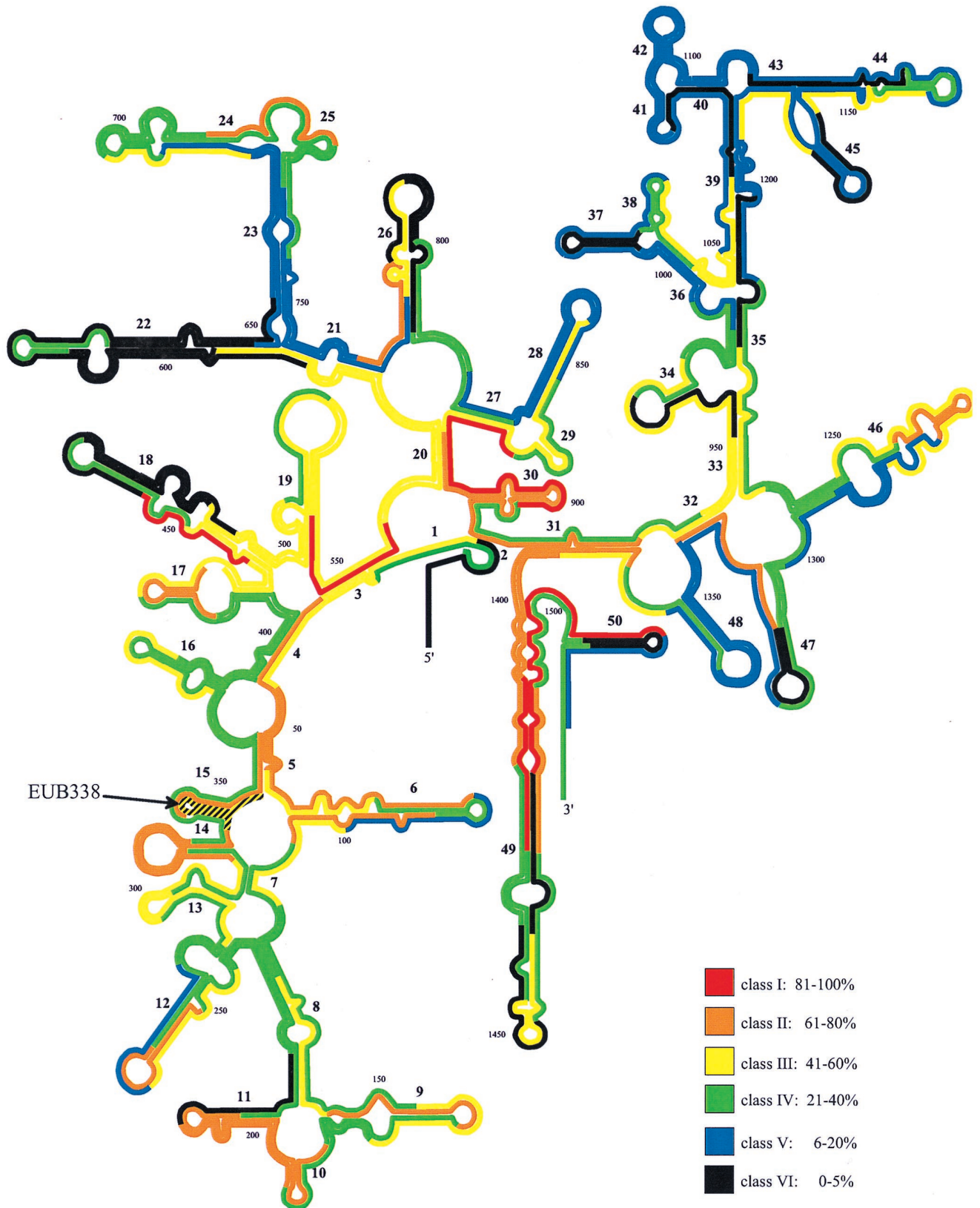
FIG. 1. Probe-conferred fluorescence for nine selected probes at various hybridization stringencies. All hybridizations were performed at 46°C. The theoretical temperatures of 36 and 41°C were achieved by increasing the [NaCl]; those of 51, 56, 66, and 76°C were achieved by addition of formamide (see Materials and Methods).

Eco952, Eco1060, Eco1113, Eco1202, Eco1437, and Eco1464. Target regions which are apparently only partially accessible to oligonucleotides (class V) include the loop regions of helix 6; almost the full lengths of helices 23, 41, 42, and 48; the 5' halves of helices 27, 28, 36, and 38; parts of helices 39, 40, 43, and 44; the 3' halves of helices 12, 21, 35, 46, 47, and 50; and the proximal stem of helix 45.

High-resolution analysis of in situ accessibility of helices 6 and 18. The two sets of adjacent probes had indicated dramatic changes in helices 6 and 18, which are among the most important target sites since they are phylogenetically less conserved. Therefore, the standard probe sets were complemented by additional probes designed with a spacing of 2 to 4 nucleotides. For helix 6 (Fig. 3A) it could be demonstrated that the signal

intensity dropped from 48% for Eco70 to 3% for Eco79. An even steeper change occurs within 4 nucleotides between Eco87 (10%), Eco89 (41%), and Eco91 (70%). These results suggest that the loop region of helix 6 is not very accessible compared to the double-stranded stem region. Similar results were obtained for helix 18 (Fig. 3B), where the signal drops from over 80% (Eco440) to background fluorescence at position 455 and rises again from 20% for Eco478 to 60% for Eco484. Here again, the loop region and the distal 3' side of the helix are not accessible.

High-resolution analysis of in situ accessibility of positions 621 to 693. One of the most frequently used target regions for 16S rRNA-targeted probe design was the 5' half of helix 23, which has yielded numerous bright oligonucleotides specific at



Downloaded from <http://aem.asm.org/> on October 23, 2019 by guest

FIG. 2. Distribution of relative fluorescence intensities of oligonucleotide probes, standardized to that of the brightest probe, Eco1482, on a 16S rRNA secondary structure model (12). The two overlapping sets of adjacent oligonucleotides, not the fine mapping, are shown. Different colors indicate different brightness classes (I through VI).

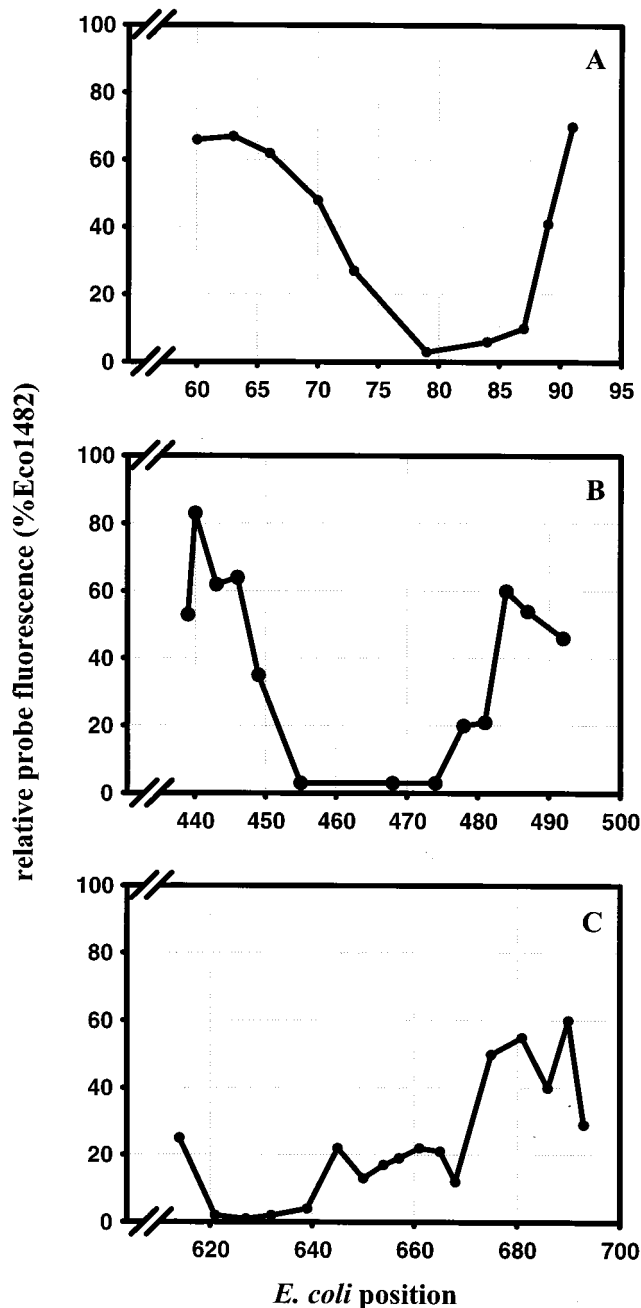


FIG. 3. Detailed analysis of three evolutionarily less conserved regions. (A) Helix 6; (B) helix 18; (C) 3' half of helix 22 and 5' halves of helices 23 and 24. Oligonucleotide probes in addition to the standard probe set were designed to increase the resolution. All fluorescence intensities were standardized to that of the brightest probe, Eco1482.

the genus level (4). Since the signals obtained for *E. coli* in this region were surprisingly low, we supplemented the standard sets with additional probes targeting the 3' half of helix 22 and the 5' halves of helices 23 and 24, with a spacing of about 5 nucleotides. The results (Fig. 3C) corroborated our initial findings. Probes Eco645 through Eco668 gave relative intensities of around 20%. Interestingly, the probes complementary to the 3' half of helix 22 (Eco621 to Eco639) yielded only background fluorescence (1 to 4%), whereas those beyond Eco675 were at or above 40%. To check whether the 5' half of helix 23 is more

accessible in other bacteria, three reference organisms, *A. calcoaceticus* DSM 30006^T, *Z. ramigera* ATCC 25935, and *C. testosteroni* DSM 50244^T, were reevaluated with three already published probes targeting this region: CTE23a for *C. testosteroni* (positions 659 to 676) (24), ZBE23a for *Z. ramigera* (positions 646 to 663) (22), and ACA23a for *A. calcoaceticus* (positions 652 to 669) (30). To compensate for potential differences in the rRNA content and the permeability of the different reference cells, all signals were normalized to the signal obtained for probe EUB338. Probes CTE23a and ZBE23a yielded signals about twice as bright as that with EUB338, and ACA23a was even three times brighter, when hybridized to the respective target cells. In contrast, probes Eco645 through Eco661, targeting the corresponding positions in helix 23 of *E. coli*, showed only about one-third of the signal of EUB338.

DISCUSSION

The objective of this study was to generate a map of the accessibility of the 16S rRNA of *E. coli* for fluorescently labeled oligonucleotide probes. It was therefore critical that the probe-mediated fluorescence was not affected by other parameters, such as differences in the probe quality or dissociation temperature, to name only the two most important ones. We consequently performed a rigid quality control, accepting for this study only probes purified by high-pressure liquid chromatography and labeled with carboxyfluorescein by the highly effective solid-phase synthesis with A_{260}/A_{496} ratios that were close to the ratio (260 versus 496 nm) of theoretical extinction coefficients. On the other hand, we could not determine optimal hybridization conditions for each individual probe. Even with the unsurpassed speed of flow cytometric quantification of fluorescence intensities, such an analysis of all 200 probes was beyond the reach of this study. We consequently applied all probes under standardized conditions. This also means that the quality of our data relies on two assumptions: (i) a sigmoidal behavior of probe binding over stringency and (ii) the accuracy of the 4+2 formula in estimating the dissociation temperature. In order to evaluate the plausibility of our assumptions, we tested nine probes at different hybridization temperatures and stringencies in an early phase of the experiment. Seven probes had optimal signals at 46°C, but two probes showed maximum fluorescence at 41°C despite estimated melting points of about 50°C. Nevertheless, we did not change the standard hybridization conditions, since the assumption of a roughly sigmoidal shape of the stringency-binding curve also did not hold for some probes. As reported before (5), binding at close to but below the temperature of dissociation can be higher than that at lower stringencies. It has been speculated that this might be due to changes in the accessibility of target sites under different hybridization conditions. Since hybridization at 46°C yielded at least 80% of the maximum signal, we would like to argue here that even though we clearly cannot rule out an influence of probe-to-probe differences in optimal hybridization conditions, this effect is secondary and would change the classification of probes by at most one brightness class. Considering all factors, the fluorescent signals reported in this study for more than 200 probes should be interpreted with some care, but with the controls described above they should be reliable within $\pm 10\%$ of the fluorescence of probe Eco1482 and should reflect mainly differences in 16S rRNA accessibility.

Changes in the accessibility as shown in Fig. 2 are often steady along the primary structure of the 16S rRNA but can also be rapid and are therefore quite unpredictable. For each of the three domains of the 16S rRNA, probes of all brightness classes are present. Probes targeting domain I (Eco1 to

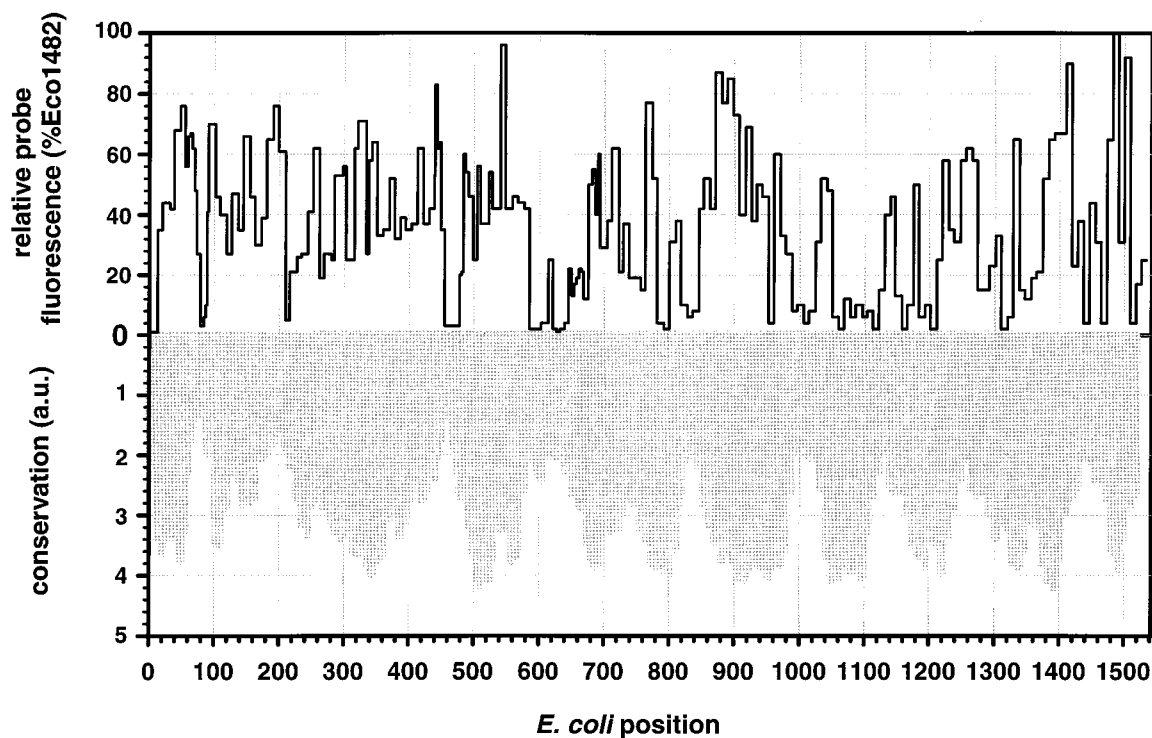


FIG. 4. Comparison of relative fluorescence (solid line) and average conservation (gray) of all probes targeted to *E. coli*. Conservation values for each probe were calculated by averaging the conservation values stated in the ARB database (27) for those positions targeted by a probe. The conservation values are based on the fractions of available bacterial sequences that have an identical nucleotide in a particular alignment position. They are expressed in arbitrary units (a.u.), where low values indicate low evolutionary conservation.

Eco541) are, with an average of 42% of the maximum fluorescence of probe Eco1482, significantly brighter than probes targeting domains II (Eco548 to Eco917) and III (Eco926 to Eco1526), with averages of 32 and 30%, respectively. Interestingly, the almost inaccessible target sites of class VI probes are frequently in the periphery of the secondary structure model (Fig. 2), including many loops, whereas regions in the center of this model seem to be more readily accessible. Since we opted at the outset of the study to use two sets of adjacent oligonucleotides of quite invariant lengths, no special care was taken to keep probes on one side of the target helix in order to avoid self-complementarity. Consequently, a lack of binding of certain of these loop-associated probes could be due to internal backfolding rather than to inaccessibility of target sites. This might apply to three probes of class VI, i.e., Eco1006, Eco1310, and Eco1506, targeting helices 37, 47, and 50, respectively. Self-complementarity of probes, however, cannot explain the clusters of class VI probes in helices 18, 22, and 26, where target site inaccessibility is found also for probes that have no self-complementarity at all.

In Fig. 4 we compare probe-conferred fluorescence values with evolutionary conservation of the respective regions of the 16S rRNA molecule. By referring to Fig. 4, it should be possible to more easily select target sites that yield both highly specific and bright probes for fluorescent in situ hybridization. Clearly, some of the most variable regions also show narrow but strong minima of in situ accessibility. This might explain the failure of many fluorescent in situ hybridization experiments. Frequently, probes were intended to be as specific as possible, targeting particular species or genera or even just particular 16S rDNA sequences that were retrieved from the environment. Those probes necessarily target the most variable regions of the 16S rRNA molecule, such as, e.g., helices 6,

18, and 22. Even though these probes might have worked nicely with extracted rRNA or as primers for PCR, no binding to whole fixed cells could be detected. The comparison of the in situ accessibility map of *E. coli* and evolutionary conservation also shows that the regions with high variability are usually wider than the zones of low accessibility. This means that a highly variable region which had appeared to be unsuitable for in situ hybridization with one peculiar probe might still be useful if the target site is shifted by several nucleotides. The effect of shifting the target sites by a few nucleotides was therefore studied in greater detail for the three evolutionarily less conserved helices, helices 6, 18, and 23.

Helix 18 showed quite dramatic changes in accessibility. Since we assume that what was measured for *E. coli* in terms of in situ accessibility would to a large degree also apply to other species, it is interesting to compare our results to other findings. Probe Nsv443, specific for the genera *Nitrosolobus*, *Nitrospira*, and *Nitrosovibrio* of the chemolithotrophic, ammonia-oxidizing bacteria of the beta subclass of the class *Proteobacteria*, gives bright in situ signals (19), whereas a probe with similar specificity, Nsp452, could be used only as a PCR primer (21) and did not work for fluorescent in situ hybridization (21a). The results of our detailed study of helix 18 in *E. coli* are in line with this observation. Eco440 is in class I, whereas Eco455 is in class VI, showing not much more than background fluorescence.

As for helix 18, the accessibility of helix 6 is quite high in the proximal stem region between probes Eco60 and Eco70 in the 5' half and probes Eco89 and Eco91 in the 3' half. Accessibility of the distal part of this helix, including the loop, is much lower, with relative intensities of Eco79, Eco84, and Eco87 of only 3, 6, and 10%, respectively. Here, only probe Eco79 has some self-complementarity (the four 3' nucleotides could fold

back), whereas Eco84 and Eco87 target only the loop and the 3' half of the helix, thereby excluding self-complementarity as the major reason for the observed inaccessibility. The probe-to-probe changes in signal intensity (Table 1) for the 10 probes between Eco60 and Eco91 are gradual and allow the cause of inaccessibility in *E. coli* to be mapped quite accurately to about positions 87 to 90. This takes into account that a lack of binding near the end of a short duplex is generally less destabilizing than an internal hindrance (26). Obviously, the interactions that almost completely block binding of Eco79, Eco84, and Eco87 are restricted to a very narrow region. Interestingly, several probes that successfully target helix 6 in other bacteria exclude the region that is blocked in *E. coli* and target either the 5' half (MPA60 [*Microthrix parvicella*, positions 60 to 77] [10], AER66 [*Aeromonas* sp., positions 66 to 83] [14], Pst67 [*Pseudomonas stutzeri*, positions 67 to 84] [1], and Hau66 [*Herpetosiphon aurantiacus*, positions 66 to 84] [1a]) or the proximal part of the 3' half (ARC94, positions 94 to 111 [25]). These bacteria include both members of the gamma subclass of the class *Proteobacteria* (*Aeromonas* sp. and *P. stutzeri*), of which *E. coli* is also a member, and members of only distantly related phyla of the *Bacteria* (*H. aurantiacus* [*Chloroflexus* branch] and *M. parvicella* [a gram-positive bacterium with a high G+C content of the DNA]). Again, this is a good indication that the in situ accessibilities that we determined for *E. coli* apply to other microorganisms as well.

The same is true for probes targeting helix 22. Empirical data acquired by the testing of numerous probes for various bacteria (1a) had suggested that the second bulge on helix 22 (positions 640 to 643) could be a strong hindrance for probe binding. Our fine mapping with probes complementary to positions 621 to 656 confirms this. Eco621, Eco627, Eco632, and Eco639 show only background fluorescence, whereas Eco645, targeting the adjacent sequence, already has an increased relative fluorescence intensity of 22%. In reviews, Ehresmann et al. (9) as well as Malhorta and Harvey (18) have summarized numerous results from both cross-linking and nuclease protection assays that indicate several interactions of helix 22 with small subunit proteins S8, S16, and S17. Of special interest for our study is the interaction between protein S8 and positions 642 and 643.

Another recent report on the conformation of the 16S rRNA is also in line with our data. Lodmell and Dahlberg (16) have postulated a conformational switch in the proximal stem region of helix 30, including positions 885 to 890 and 910 to 912, that should occur during mRNA translation. This switch requires an open conformation in the vicinity, and we indeed found good accessibility of helix 30 and other core regions. With the large amount of data presented in our study, this type of speculation could be continued. However, we have to state here again that our primary goal was mapping of 16S rRNA in situ probe accessibility and not an analysis of the higher-order structure of the small subunit of the ribosome. One should always keep in mind that we worked on formaldehyde-fixed *E. coli* cells with 18-mers that necessarily integrate accessibility over larger regions. Nevertheless, we hope that our data will be of interest to experts in the field of ribosome conformation.

The only major unexpected finding in our study was the low accessibility of the 5' half of helix 23. About one-quarter of the >200 probes developed in our laboratory over the last 8 years target this region (see, e.g., reference 4). There are two reasons for this: first, the variability of the nucleotides in this region makes it easy to find signature sequences on about the genus level, and second, the accessibility was in most cases very high, yielding bright fluorescence signals. However, the quantification of probes targeting the 5' half of helix 23 of *E. coli* DSM

30083^T yielded values of between only 12 and 23% of the signal of probe Eco1482. Flow cytometric quantification of the signals conferred by probes targeting this helix in three other species, *A. calcoaceticus*, *Z. ramigera*, and *C. testosteroni*, clearly demonstrated that the in situ accessibility of helix 23 is indeed generally very good. Obviously, for this particular region *E. coli* is a bad model for other organisms. Even though the 16S rRNA is a highly conserved molecule, there are differences in the primary and higher-order structures that will be more pronounced the more distantly related two organisms are. Certain probe target sites that are considered to be open in most species can be deleted in certain species, and obviously, from our *E. coli* map nothing can be deduced about the accessibility of insertions that are present in other phyla.

With these limitations for the transferability of our *E. coli* data to other species, there is still a clear need to test every newly developed probe on reference organisms before it is used with natural samples for the quantification and in situ localization of individual cells. However, we hope that this publication will contribute to a higher probability of successful design of oligonucleotide probes for in situ hybridization.

ACKNOWLEDGMENTS

This study was supported by grants from the DFG (Am73/2-4), the BMBF (21P1624), and the Max Planck Society.

The technical assistance of Sibylle Schadhauer and Maik Schwerdtfeger is acknowledged.

REFERENCES

- Amann, R., W. Ludwig, R. Schulze, S. Spring, E. Moore, and K. H. Schleifer. 1996. rRNA-targeted oligonucleotide probes for the identification of genuine and former pseudomonads. *Syst. Appl. Microbiol.* **19**:501-509.
- Amann, R. Unpublished results.
- Amann, R. I., B. J. Binder, R. J. Olson, S. W. Chisholm, R. Devereux, and D. A. Stahl. 1990. Combination of 16S rRNA-targeted oligonucleotide probes with flow cytometry for analyzing mixed microbial populations. *Appl. Environ. Microbiol.* **56**:1919-1925.
- Amann, R. I., L. Krumholz, and D. A. Stahl. 1990. Fluorescent-oligonucleotide probing of whole cells for determinative, phylogenetic, and environmental studies in microbiology. *J. Bacteriol.* **172**:762-770.
- Amann, R. I., W. Ludwig, and K. H. Schleifer. 1995. Phylogenetic identification and in situ detection of individual microbial cells without cultivation. *Microbiol. Rev.* **59**:143-169.
- Amann, R. I., J. Stromley, R. Devereux, R. Key, and D. A. Stahl. 1992. Molecular and microscopic identification of sulfate-reducing bacteria in multispecies biofilms. *Appl. Environ. Microbiol.* **58**:614-623.
- Beisker, W. 1994. A new combined integral-light and slit-scan data analysis system (DAS) for flow cytometry. *Comput. Prog. Biomed.* **42**:15-26.
- Brosius, J., T. J. Dull, D. D. Sleeter, and H. F. Noller. 1981. Gene organization and primary structure of a ribosomal RNA operon from *Escherichia coli*. *J. Mol. Biol.* **148**:107-127.
- DeLong, E. F., G. S. Wickham, and N. R. Pace. 1989. Phylogenetic stains: ribosomal RNA-based probes for the identification of single cells. *Science* **243**:1360-1363.
- Ehresmann, B., C. Ehresmann, P. Romby, M. Mougel, F. Baudin, E. Westhof, and J.-P. Ebel. 1990. Detailed structures of rRNAs: new approaches, p. 148-159. In W. E. Hill, A. Dahlberg, R. A. Garrett, P. B. Moore, D. Schlessinger, and J. R. Warner (ed.), *The ribosome: structure, function, and evolution*. American Society for Microbiology, Washington, D. C.
- Erhart, R., D. Bradford, R. J. Seviour, R. Amann, and L. L. Blackall. 1997. Development and use of fluorescent in situ hybridization probes for the detection and identification of "*Microthrix parvicella*" in activated sludge. *Syst. Appl. Microbiol.* **20**:310-318.
- Frischer, M. E., P. J. Floriani, and S. A. Nierzwicki-Bauer. 1996. Differential sensitivity of 16S rRNA targeted oligonucleotide probes used for fluorescence in situ hybridization is a result of ribosomal higher order structure. *Can. J. Microbiol.* **42**:1061-1071.
- Gutell, R. R. 1994. Collection of small subunit (16S- and 16S-like) ribosomal RNA structures: 1994. *Nucleic Acids Res.* **22**:3502-3507.
- Hill, W. E., J. Weller, T. Gluick, C. Merryman, R. T. Marconi, A. Tassanakajohn, and W. E. Tapprich. 1990. Probing ribosome structure and function by using short complementary DNA oligomers, p. 253-264. In W. E. Hill, A. Dahlberg, R. A. Garrett, P. B. Moore, D. Schlessinger, and J. R. Warner (ed.), *The ribosome: structure, function, and evolution*. American Society for Microbiology, Washington, D. C.

14. **Kämpfer, P., R. Erhart, C. Beimfohr, J. Böhringer, M. Wagner, and R. Amann.** 1996. Characterization of bacterial communities from activated sludge: culture-dependent numerical identification versus in situ identification using group- and genus-specific rRNA-targeted oligonucleotide probes. *Microb. Ecol.* **32**:101–121.
15. **Lasater, L. S., H. McKuskie Olson, P. A. Cann, and D. G. Glitz.** 1988. Complementary oligodeoxynucleotide probes of RNA conformation within the *Escherichia coli* small ribosomal subunit. *Biochemistry* **27**:4687–4695.
16. **Lodmell, J. S., and A. E. Dahlberg.** 1997. A conformational switch in *Escherichia coli* 16S ribosomal RNA during decoding of messenger RNA. *Science* **277**:1262–1267.
17. **Maidak, B. L., G. J. Olsen, N. Larsen, R. Overbeek, M. J. McCaughey, and C. R. Woese.** 1997. The RDP (Ribosomal Database Project). *Nucleic Acids Res.* **25**:109–111.
18. **Malhorta, A., and S. C. Harvey.** 1994. A quantitative model of the *Escherichia coli* 16S RNA in the 30 S ribosomal subunit. *J. Mol. Biol.* **240**:308–340.
19. **Mobarry, B. K., M. Wagner, V. Urbain, B. E. Rittman, and D. A. Stahl.** 1996. Phylogenetic probes for analyzing abundance and spatial organization of nitrifying bacteria. *Appl. Environ. Microbiol.* **62**:2156–2162.
20. **Olsen, G. J., D. J. Lane, S. J. Giovannoni, N. R. Pace, and D. A. Stahl.** 1986. Microbial ecology and evolution: a ribosomal rRNA approach. *Annu. Rev. Microbiol.* **40**:337–365.
21. **Pommerening-Röser, A., G. Rath, and H.-P. Koops.** 1996. Phylogenetic diversity within the genus *Nitrosomonas*. *Syst. Appl. Microbiol.* **19**:344–351.
- 21a. **Rath, G.** Personal communication.
22. **Rossello-Mora, R. A., M. Wagner, R. Amann, and K.-H. Schleifer.** 1995. The abundance of *Zoogloea ramigera* in sewage treatment plants. *Appl. Environ. Microbiol.* **61**:702–707.
23. **Sambrook, J., E. F. Fritsch, and T. Maniatis.** 1989. *Molecular cloning: a laboratory manual*, 2nd ed., vol. 3, p. 11–21. Cold Spring Harbor Laboratory Press, Cold Spring Harbor, N.Y.
24. **Schleifer, K.-H., R. Amann, W. Ludwig, C. Rothemund, N. Springer, and S. Dorn.** 1992. Nucleic acid probes for the identification and in situ detection of pseudomonads, p. 127–134. *In* E. Galli, S. Silver, and B. Witholt (ed.), *Pseudomonads: molecular biology and biotechnology*. American Society for Microbiology, Washington, D.C.
25. **Snaird, J., R. Amann, I. Huber, W. Ludwig, and K.-H. Schleifer.** 1997. Phylogenetic analysis and in situ identification of bacteria in activated sludge. *Appl. Environ. Microbiol.* **63**:2884–2896.
26. **Stahl, D. A., and R. Amann.** 1991. Development and application of nucleic acid probes, p. 205–248. *In* E. Stackebrandt and M. Goodfellow (ed.), *Nucleic acid techniques in bacterial systematics*. John Wiley & Sons Ltd., Chichester, United Kingdom.
27. **Strunk, O., O. Gross, B. Reichel, M. May, S. Hermann, N. Stuckmann, B. Nonhoff, T. Ginhart, A. Vilbig, M. Lenke, T. Ludwig, A. Bode, K.-H. Schleifer, and W. Ludwig.** ARB: a software environment for sequence data. <http://www.mikro.biologie.tu-muenchen.de>. Department of Microbiology, Technische Universität München, Munich, Germany.
28. **Suggs, S. V., T. Hirose, T. Miyake, E. H. Kawashima, M. J. Johnson, K. Itakura, and R. B. Wallace.** 1981. Use of synthetic oligodeoxyribonucleotides for the isolation of specific cloned DNA sequences, p. 683–693. *In* D. Brown and C. F. Fox (ed.), *Developmental biology using purified genes*. Academic Press, Inc., New York, N.Y.
29. **Van de Peer, Y., A. Caers, P. De Rijk, and R. De Wachter.** 1998. Database on the structure of small ribosomal subunit RNA. *Nucleic Acids Res.* **26**:179–182.
30. **Wagner, M., R. Erhart, W. Manz, R. Amann, H. Lemmer, D. Wedi, and K.-H. Schleifer.** 1994. Development of an rRNA-targeted oligonucleotide probe specific for the genus *Acinetobacter* and its application for in situ monitoring in activated sludge. *Appl. Environ. Microbiol.* **60**:792–800.
31. **Wallner, G., R. Amann, and W. Beisker.** 1993. Optimizing fluorescent in situ hybridization with rRNA-targeted oligonucleotide probes for flow cytometric identification of microorganisms. *Cytometry* **14**:136–143.
32. **Wallner, G., B. Fuchs, S. Spring, W. Beisker, and R. Amann.** 1997. Flow sorting of microorganisms for molecular analysis. *Appl. Environ. Microbiol.* **63**:4223–4231.
33. **Woese, C. R.** 1987. Bacterial evolution. *Microbiol. Rev.* **51**:221–271.